

Compact High-Selectivity Dual/Tri-Band Bandpass Filters for WLAN Applications

Shance Lv, Yuehe Ge*, and Weiguo Zhang

Abstract—This paper presents compact dual/tri-band bandpass filters (BPFs) with controllable frequency and high selectivity for WLAN applications. A stepped impedance resonator with a shorting stub and a uniform impedance resonator with an open stub are applied in the designs. Several techniques that can generate transmission zeros are combined to improve the frequency selectivity. The resonators and the proposed filters are characterized by full-wave simulations. To validate the design strategies, a dual-band BPF centered at 2.4 GHz and 5.2 GHz was first designed. With a minor modification, a tri-band BPF centered at 2.4 GHz, 5.2 GHz and 5.8 GHz was then developed. Both simulations and measurements were carried out to demonstrate the effectiveness of the designs. Good agreements are achieved.

1. INTRODUCTION

Microwave multi-band filter has been an attractive issue due to the increasing demand of wireless communication systems operating in multiple separate frequency bands [1]. Many researchers' attention has been gained in recent years to develop multiband bandpass filters (BPFs) with compact size, planar configuration, and high selectivity performance. More and more dual-band and tri-band filters with various configurations appear in literatures. The stepped impedance resonators (SIR) have been well investigated and were reported to develop multiband BPFs [2–8], due to their multiband behavior, simple structure and well established design methodology. Several different resonators can be combined with a common feeding structure to obtain a multiband BPF [7]. However, such a BPF will normally have a large size. Multi-mode resonators are also proposed for multiband applications [8–10]. Flexibly controlling or tuning the passbands within the BPFs and high frequency selectivity are the basic requirements for this kind of BPFs. Therefore, controlling or generating transmission zeros is another crucial technique [11–16] for high performance multiband BPFs.

In this paper, a dual-band BPF centered at 2.4 GHz and 5.2 GHz was first developed by using two different resonators for the WLAN application. Based on it, an improved version, a tri-band BPF centered at 2.4 GHz, 5.2 GHz and 5.8 GHz was then implemented. Compared with other multiband filters based on multiple resonators, with a common feeding structure, the proposed filters have much smaller sizes. To improve the frequency selectivity of the two BPFs, a special coupling structure is utilized among the two resonators and the feedlines, resulting in five transmission zeros distributing on the upper and lower sides of the passbands. By tuning or changing the sizes of the two resonators, the passbands can be tuned or changed to other frequencies for different applications.

2. DUAL-BAND FILTER DESIGN

The configuration of the proposed dual-band BPF is shown in Fig. 1. As depicted, the dual-band BPF consists of two different resonators, with an open stub and a shorting stub, respectively. Resonator 1 is

Received 26 November 2015, Accepted 5 January 2016, Scheduled 13 January 2016

* Corresponding author: Yuehe Ge (yuehe@ieee.org).

The authors are with the College of Information Science and Engineering, Huaqiao University, Xiamen, Fujian 361021, China.

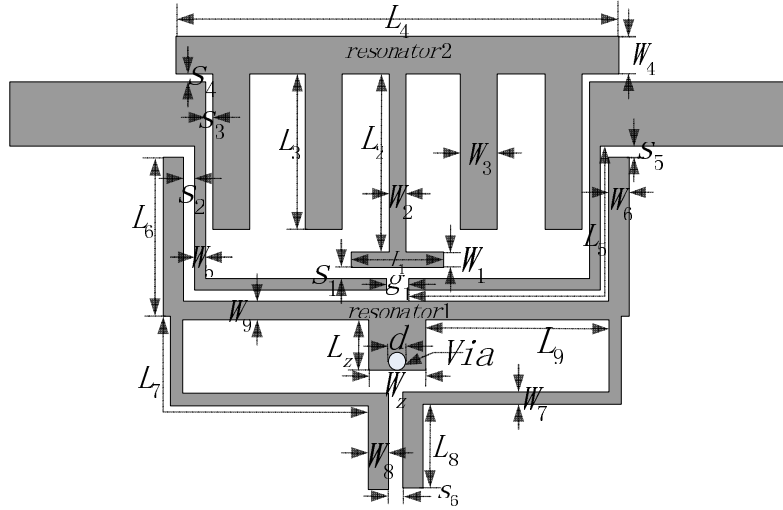


Figure 1. Layout of the proposed dual-band BPF.

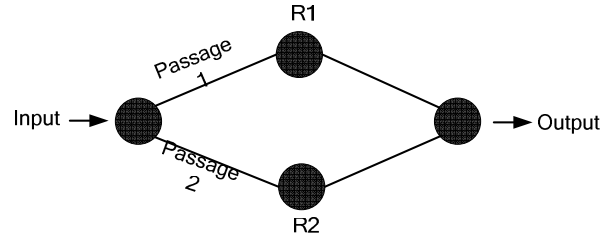


Figure 2. Coupling structure of the proposed dual-band BPF.

based on the SIR with a shorting stub, while Resonator 2 is based on the uniform impedance resonator (UIR) with an open stub. The coupling structure is located between the two resonators. Fig. 2 shows the coupling or the transmission structure of the dual-band BPF, where R_1 and R_2 represent Resonators 1 and 2, respectively. Passages 1 and 2 stand for the two passbands respectively.

Both resonators can be initially considered as a microstrip half-wavelength resonator with an open stub and that with a shorting stub, as shown in Figs. 3(a) and 3(b) respectively, which can be theoretically characterized using the theory of even/odd-mode analyses, as detailed in [13]. In this paper, the two standard resonators have been modified so that high selectivity or more transmission zeros can be obtained in the proposed BPFs. The characterization of the two modified resonators will be carried out using the Ansys HFSS.

The two modified resonators were first characterized separately, using the coupling structure shown in Fig. 1. The two passbands under consideration are centered at 2.4 GHz and 5.2 GHz, respectively. The substrate applied to the study has a thickness of 0.8 mm and a relative dielectric constant of 2.55. After the initial study, the values of the filter parameters, shown in Fig. 1, are: $L_1 = 3.5$ mm, $L_2 = 6.5$ mm, $L_3 = 6$ mm, $L_4 = 15$ mm, $L_5 = 12.0$ mm, $L_6 = 5$ mm, $L_7 = 9.5$ mm, $L_8 = 3$ mm, $L_9 = 6.5$ mm, $L_z = 1.5$ mm, $W_1 = 0.4$ mm, $W_2 = 0.5$ mm, $W_3 = 0.9$ mm, $W_4 = 0.9$ mm, $W_5 = 0.5$ mm, $W_6 = 0.6$ mm, $W_7 = 0.3$ mm, $W_8 = 0.8$ mm, $W_9 = 0.65$ mm, $W_z = 1.5$ mm, $s_1 = 0.3$ mm, $s_2 = 0.2$ mm, $s_3 = 0.3$ mm, $s_4 = 0.2$ mm, $s_5 = 0.3$ mm, $s_6 = 0.4$ mm, $d = 0.4$ mm, $g_1 = 0.4$ mm. All the simulations in this section are based on the above parameter values. Figs. 4(a) and 4(b) shows the simulated reflection and transmission coefficients of a filter only containing Resonator 1 and 2, respectively. The filter structures under characterization are shown as the inset in Figs. 4(a) and 4(b) respectively. It can be seen that passbands centered at 2.5 GHz and 5.6 GHz are generated over the frequency band concerned in Figs. 4(a) and 4(b) respectively, demonstrating the effectiveness of the two resonators. The two resonators were then combined to construct a dual-band filter using the same coupling structure, as shown in Fig. 1. Fig. 5(a) shows the simulated frequency responses for the proposed dual-band

filter. The parametric study was also carried out. Fig. 5(a) also shows the results of the filter when changing the length L_1 of the open stub. As can be seen, the second passband can be shifted within an appropriate range while the first passband is not affected by changing parameter L_1 . To illustrate the frequency shifting clearly, the frequency responses in the upper band are plotted separately in Fig. 5(b). Similar phenomena can be obtained for the first passband when varying the length of the shorting stub. Therefore, the required two passbands can be obtained using the proposed filter.

The methods of generating transmission zeros were also studied and applied to the proposed filter. Four techniques in total are considered. The first is the use of a pseudo interdigital resonator, which is applied to Resonator 2. The second is to change the position of the high order harmonic to generate transmission zeros by appropriately folding the transmission line, as shown in Resonator 1. It can be seen in Fig. 4(a) that two transmission zeros are generated by appropriately folding the transmission line, much improving the frequency selectivity of the dual-band BPF. The third is that the direct-coupling

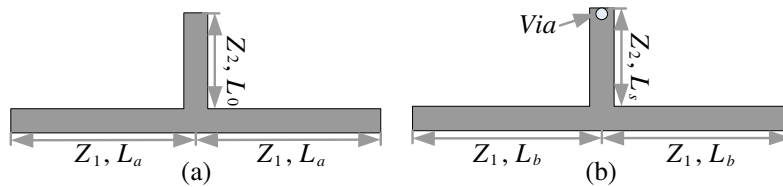


Figure 3. (a) The open stub-loaded resonator; (b) the shorting stub-loaded.

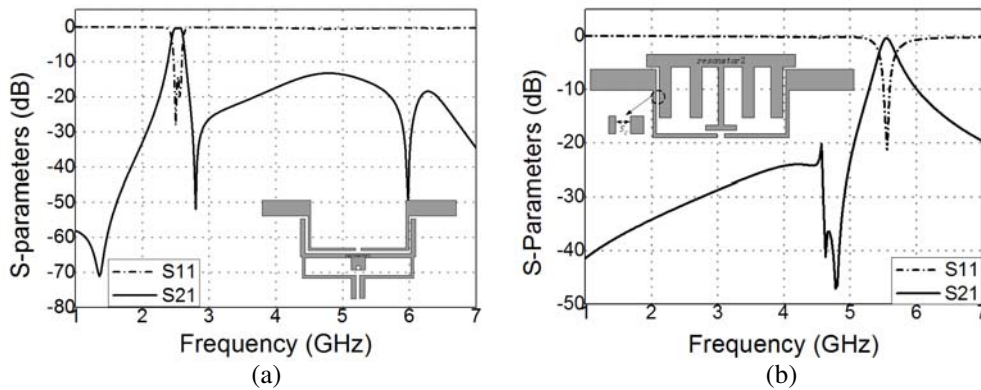


Figure 4. (a) The simulated reflection and transmission coefficients of the filter with only Resonator 1; (b) the simulated reflection and transmission coefficients of the filter with only Resonator 2.

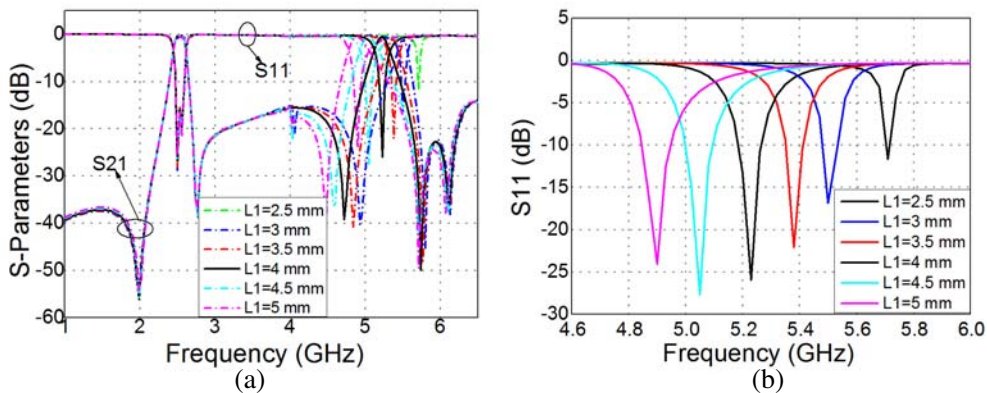


Figure 5. Simulated reflection and transmission coefficients against L_1 for the proposed dual-band BPF in: (a) the overall band; (b) the upper band.

between the two resonators or the direct-coupling between the source and the load. These can produce two or three transmission zeros. By increasing the length of the source line and load line, the direct-coupling between the source and the load is increased. Due to the coupling among the feedlines and the resonators, the transmission path is extended, resulting in more transmission zeroes and improving the transmission characteristics of the passbands. The last is to load an open or a shorting stub to produce transmission zeros. Note that the loading stubs should not be too long, otherwise it will cause unnecessary coupling.

Here the first method was tested numerically. As shown in Fig. 6(a), the simulated transmission coefficients of the dual-band BPFs, with and without the pseudo interdigital stubs, have different transmission zeros. Two more transmission zeros are observed for the result of the BPF with the pseudo interdigital stubs, making it possessing the better frequency selectivity in the operating band. Fig. 6(b) shows the transmission coefficients of the dual-band BPFs with and without the shorting stub. It can be seen that more transmission zeros are obtained for the BPF with a shorting stub.

The proposed filter comprehensively utilizes the above four methods. As expected and shown in Fig. 5, five transmission zeros are generated in the design, which greatly improve the frequency selectivity of the filter.

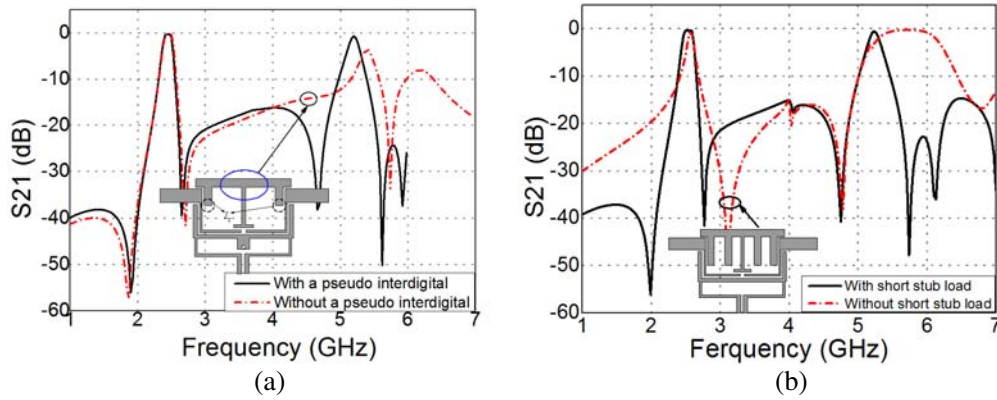


Figure 6. (a) Transmission coefficients of the dual-band BPF with/without pseudointerdigital stubs; (b) transmission coefficients of the dual-band BPF with/without a short stub load.

Finally, a dual-band BPF centered at 2.4 GHz and 5.2 GHz was designed. The proposed filter is implemented on a substrate having a thickness of 0.8 mm and a relative dielectric constant of 2.55. The full-wave commercial software Ansys HFSS was applied to tune and optimize the designed filter. The realized final parameters are: $L_1 = 3.6$ mm, $L_2 = 6.5$ mm, $L_3 = 6$ mm, $L_4 = 15$ mm, $L_5 = 12.2$ mm, $L_6 = 5$ mm, $L_7 = 9.7$ mm, $L_8 = 3$ mm, $L_9 = 6.85$ mm, $L_z = 1.5$ mm, $W_1 = 0.4$ mm, $W_2 = 0.5$ mm, $W_3 = 0.9$ mm, $W_4 = 0.9$ mm, $W_5 = 0.5$ mm, $W_6 = 0.6$ mm, $W_7 = 0.3$ mm, $W_8 = 0.8$ mm, $W_9 = 0.65$ mm, $W_z = 1.5$ mm, $s_1 = 0.3$ mm, $s_2 = 0.2$ mm, $s_3 = 0.3$ mm, $s_4 = 0.2$ mm, $s_5 = 0.3$ mm, $s_6 = 0.4$ mm, $d = 0.4$ mm, $g_1 = 0.4$ mm. The full size of the filter is 16 mm \times 16 mm, approximately $0.2\lambda_g \times 0.2\lambda_g$, where λ_g is the guided wavelength at the center frequency of the first passband. Thus, this filter is very compact.

A prototype, shown in Fig. 7, was fabricated and tested. Both simulation and measurement results are illustrated in Fig. 8(a), for comparison. To illustrate the passbands clearly, the frequency responses of the results are plotted in the two passbands separately in Fig. 8(b). As can be seen, the agreements between them are very well. The center frequencies of the two passbands are about 2.4 GHz and 5.2 GHz, respectively. The return losses in the two passbands, from both simulations and measurements, are better than 15 dB. The simulated insertion losses are about 0.3 dB and 0.8 dB at the first and second passbands, respectively, with the fractional bandwidths of about 7.4% (2.35–2.53 GHz) and 4% (5.15–5.36 GHz), respectively, while measured ones are 0.9 dB and 1.2 dB for the two bands, respectively, with the bandwidths of about 4.5% (2.39–2.5 GHz) and 4.6% (5.12–5.36 GHz), respectively. In addition, five transmission zeros are located respectively at 1.78 GHz, 2.65 GHz, 4.69 GHz, 5.58 GHz and 5.86 GHz, much improving the frequency selectivity and the isolation of the dual-band BPF.

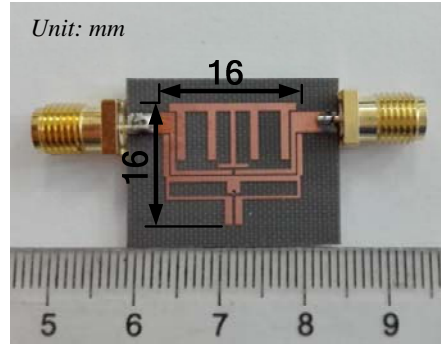


Figure 7. Prototype of the dual-band BPF.

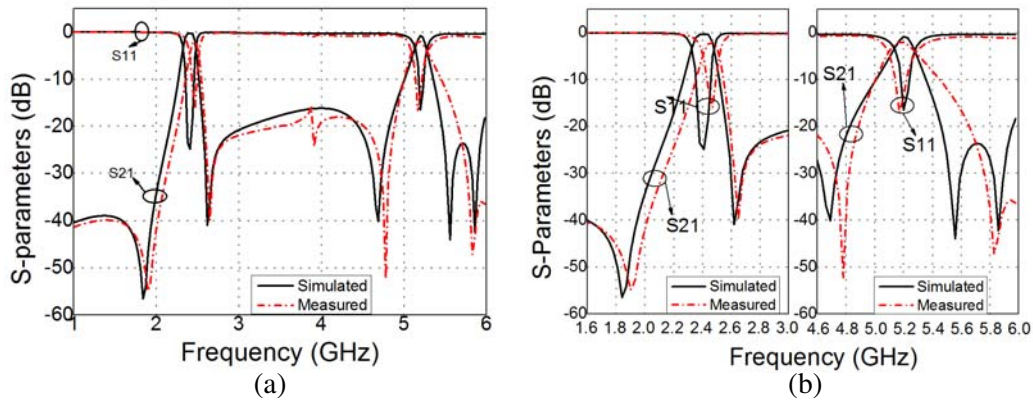


Figure 8. Simulated and measured S parameters of the dual-band BPF in: (a) the overall band; (b) the lower and the upper passbands respectively.

3. TRI-BAND FILTER DESIGN

Based on the above dual-band BPF, a tri-band BPF was further developed for WLAN applications. In this case, the second resonant mode of Resonator 1 is excited and hence it resonates at dual modes. The configuration of the proposed tri-band BPF is shown in Fig. 9. Compared with the dual-band one, two identical stubs are symmetrically loaded on the source and load transmission lines. As shown in Fig. 9, the loading stubs surround the two ports of Resonator 1, together with the source and load coupling lines. Here the results in Fig. 4(a), which only exhibits a single resonant mode, was tested again. In this case, two identical stubs are symmetrically loaded on the source and load transmission lines, as shown in the inset of Fig. 10. The simulated results, shown in Fig. 10, exhibit that the second resonant mode is excited, demonstrating that the new coupling structure and Resonator 1 exhibit a dual-mode operation. Due to the second mode resonates at a frequency close to 6 GHz, a tri-band BPF centered at 2.4 GHz, 5.2 GHz and 5.8 GHz are expected for the WLAN application. After combining the new dual-mode resonator with Resonator 2 to construct a new BPF, which has the configuration shown in Fig. 9, a tri-band BPF result was achieved and plotted in Fig. 11. It can be seen that the third passband can be obtained by loading two identical stubs on the source and load transmission lines, symmetrically on the two sides of Resonator 1, while the positions of the original two passbands will not change. Through varying the length (L_t) of the two stubs, the third passband can be minor tuned, as depicted in Fig. 11. In the design, most dimensions of the tri-band BPF are the same as those of the previous dual-band one, except for those of the two loading stubs and the width of the coupling lines. In the final design, we have $L_t = 6$ mm, $W_t = 0.7$ mm, $S_t = 0.2$ mm, and $W'_5 = 0.6$ mm. To clearly illustrate the tri-band BPF result, the current distributions on the BPF at the three resonant frequencies

2.4 GHz, 5.2 GHz and 5.8 GHz are plotted in Fig. 12 respectively, which clearly demonstrate that the strong current, representing the strong resonance, appears on Resonator 1 at 2.4 GHz, Resonator 2 at 5.2 GHz and both Resonator 1 and the two loading stubs at 5.8 GHz.

A prototype of the tri-band BPF was also fabricated for testing, whose photograph is shown in Fig. 13. The simulated and measured reflection and transmission coefficients are plotted in Fig. 14(a). The frequency responses of the reflection and transmission coefficients in the three passbands are also shown separately in Fig. 14(b), to give a clear illustration. Good agreements between the simulations and the measurements are also obtained. Three passbands, all with sharp rejection, are realized by properly adjusting the location of transmission zeros. The simulated 3-dB bandwidths of the passbands

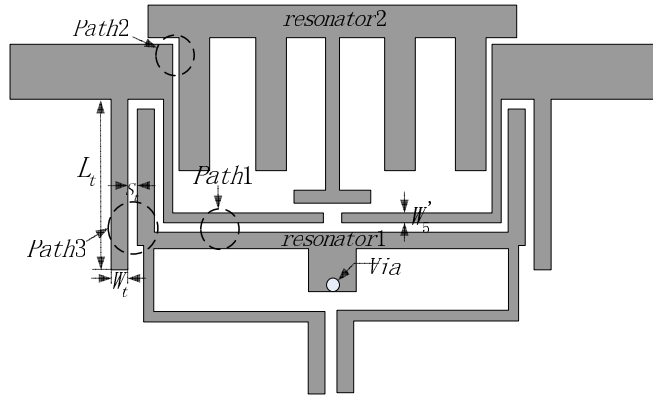


Figure 9. Layout of the proposed tri-band BPF.

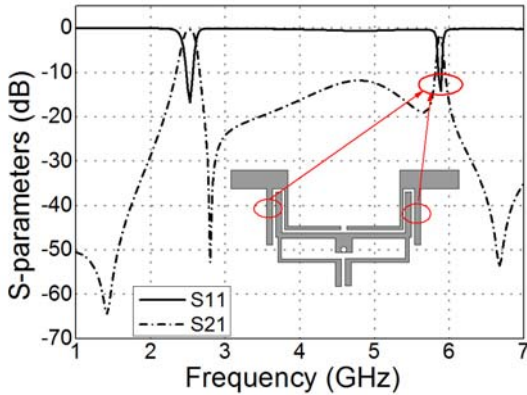


Figure 10. The reflection and transmission coefficients of the BPF with only Resonator 1 and stubs loaded on the source and load transmission lines.

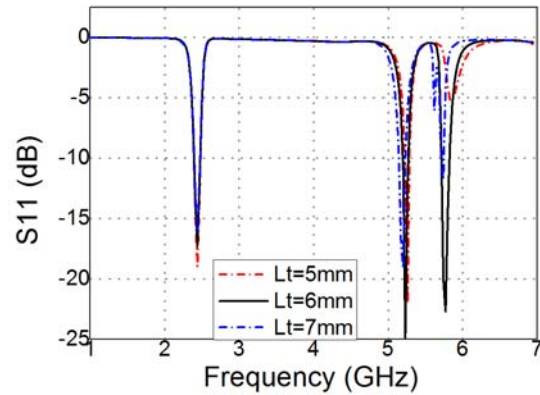


Figure 11. Simulated S_{11} against L_t for the proposed tri-band BPF.

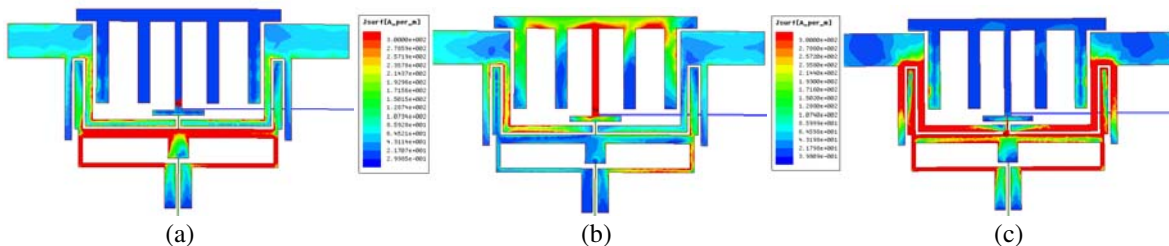


Figure 12. Current distributions: (a) at 2.4 GHz, (b) at 5.2 GHz, (c) at 5.8 GHz.

centered at 2.4 GHz, 5.2 GHz and 5.8 GHz are 2.35–2.53 GHz (7.5%), 5.15–5.36 GHz (4%) and 5.7–5.9 GHz (3.4%), respectively. The simulated return losses in the three passbands are better than 20 dB, while the simulated insertion losses are about 0.4 dB, 0.8 dB and 0.6 dB, respectively. The measured 3-dB bandwidths of the passbands centered 2.47 GHz, 5.14 GHz and 5.8 GHz are 2.41–2.56 GHz (6%), 5.02–5.38 GHz (7%), 5.71–5.95 GHz (4.1%), respectively, the measured return losses in the three passbands are better than 14 dB, and the measured insertion losses are about 1.8 dB, 1.67 dB and 2 dB at the three passbands, respectively.

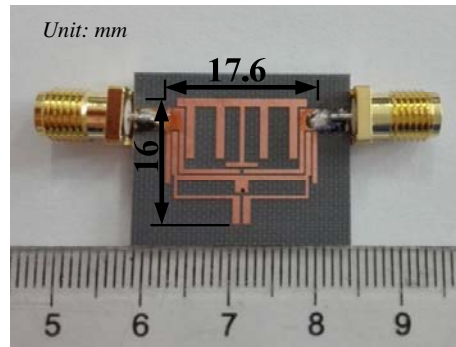


Figure 13. Prototype of the tri-band BPF.

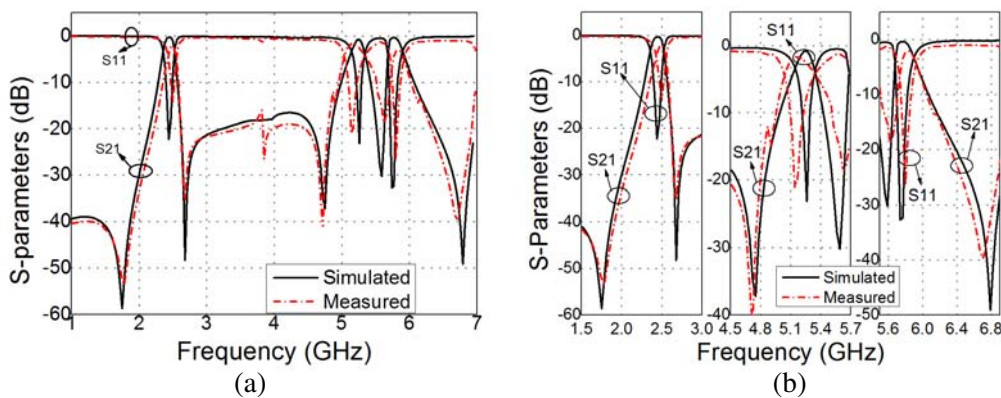


Figure 14. Simulated and measured reflection and transmission coefficients of the tri-band BPF in: (a) the overall band; (b) the separate passbands.

4. CONCLUSIONS

Compact dual/tri-band BPFs for WLAN applications, based on two resonators, were successfully developed, fabricated and tested. By appropriately arranging the two resonators and the source and load transmission coupling lines, a dual-band BPF centered at 2.4 GHz and 5.2 GHz was obtained. Through further symmetrically loading two stubs on the source and transmission lines, the third passband can be obtained, without affecting the original two passbands, and hence a tri-band BPF centered at 2.4 GHz, 5.2 GHz and 5.8 GHz for the WLAN application was achieved. To improve the performance of the frequency selectivity, four techniques in total are applied to the designs, resulting in five transmission zeros. Good agreements between simulations and measurements are achieved, demonstrating the effectiveness of the designs. The measured maximum insertion losses were better than 1.2 dB for the dual-band BPF and 2 dB for the tri-band BPF, with return losses better than 14 dB and sizes about $0.2\lambda_g \times 0.2\lambda_g$ for both BPFs. As a result, compact and high-selectivity dual/tri-band BPFs for WLAN application are successfully developed.

ACKNOWLEDGMENT

This research was supported by the Start-Up Program (11BS301) from Huaqiao University, China, Quanzhou Science and Technology Project (Z1424008), Quanzhou, Fujian province, China, and Subsidized Project for Cultivating Postgraduates' Innovative Ability in Scientific Research of Huaqiao University (1400201026).

REFERENCES

1. Ma, D. C., Z. Y. Xiao, L. L. Xiang, X. H. Wu, C. Y. Huang, and X. Kou, "Compact dual-band bandpass filter using folded SIR with two stubs for WLAN," *Progress In Electromagnetics Research*, Vol. 117, 357–364, 2011.
2. Chen, C.-F., T.-Y. Huang, and R.-B. Wu, "Design of dual- and tri-passband filters using alternately cascaded multiband resonators," *IEEE Trans. Microw. Theory Tech.*, Vol. 54, No. 9, 3550–3558, Sept. 2006
3. Lee, C.-H., C.-I. G. Hsu, and H.-K. Jhuang, "Design of a new tri-band microstrip BPF using combined quarter-wavelength SIRs," *IEEE Microw. Wireless Compon. Lett.*, Vol. 16, No. 11, 594–596, Nov. 2006
4. Lin, X.-M. and Q.-X. Chu, "Design of triple-band bandpass filter using tri-section stepped-impedance resonators," *ICMMT Int. Microwave Tech. Conf.*, 111–114, Nov. 2014
5. Hsu, C.-I. G., C.-H. Lee, and Y.-H. Hsieh, "Tri-band bandpass filter with sharp passband skirts designed using tri-section SIRs," *IEEE Microw. Wireless Compon. Lett.*, Vol. 18, No. 1, 19–21, Jan. 2008
6. Weng, M.-H., S.-K. Liu, H.-W. Wu, and C.-H. Hung, "A dual-band bandpass filter having wide and narrow bands simultaneously using multilayered stepped impedance resonators," *Progress In Electromagnetics Research Letters*, Vol. 13, 139–147, 2010.
7. Chu, Q. X., F. C. Chen, Z. H. Tu, and H. Wang, "A novel crossed resonator and its applications to bandpass filters," *IEEE Trans. Microw. Theory Tech.*, Vol. 57, No. 7, 1753–1759, June. 2009
8. Velazquez-Ahumada, M. D. C., J. Martel-Villagr, F. Medina, and F. Mesa, "Application of stub loaded folded stepped impedance resonators to dual band filter design," *Progress In Electromagnetic Research*, Vol. 102, 107–124, 2010.
9. Chen, F. C., Q. X. Chu, and Z. H. Tu, "Tri-band bandpass filter using stub loaded resonators," *Electron. Lett.*, Vol. 44, No. 12, 747–749, June. 2008
10. Quendo, C., E. Rius, and C. Person, "Narrow bandpass filter using dual-behavior resonators based on stepped-impedance stubs and different-length stubs," *IEEE Trans. Microw. Theory Tech.*, Vol. 52, No. 3, 1034–1044, Mar. 2004
11. Lee, J.-R., J.-H. Cho, and S.-W. Yun, "New compact bandpass filter using microstripl4 resonators with open stub inverter," *IEEE Microw. Guided Wave Lett.*, Vol. 10, No. 12, 526–527, Dec. 2000.
12. Gan, H., D. W. Lou, and D. X. Yang, "Compact microstrip bandpass filter with sharp transition bands," *IEEE Microw. Wireless Compon. Lett.*, Vol. 16, No. 3, 107–109, Mar. 2006
13. Zhang, X. Y., J.-X. Chen, Q. Xue, and S.-M. Li, "Dual-band filters using stub-loaded resonators," *IEEE Microw. Wireless Common. Lett.*, Vol. 17, No. 8, 583–585, Aug. 2007.
14. Zhang, X. Y., C. H. Chan, Q. Xue, and B.-J. Hu, "Dual-band bandpass filters with controllable bandwidths using two coupling paths," *IEEE Microw. Wireless Common. Lett.*, Vol. 20, No. 11, 616–618, Aug. 2010
15. Kazerooni, M. and A. Cheldavi, "Simulation, analysis, design and applications of array defected microstrip structure (ADMS) filters using rigorously coupled multi-strip (RCMS) method," *Progress In Electromagnetics Research*, Vol. 63, 193–207, 2006.
16. Khalaj-Amirhosseini, M., "Microwave filters using waveguides filled by multi-layer dielectric," *Progress In Electromagnetics Research*, Vol. 66, 105–110, 2006.